Landmarks in Earth Reinforcement, Ochiai et al. (eds),
© 2001 Swets & Zeitlinger, ISBN 90 2651 863 3

Use of a 1g geogrid reinforced-wall model to evaluate the effectiveness of a FE numerical code

M. Schiavo & P. Simonini
IMAGE, University of Padova, Italy

G. Gottardi & L. Tonni
DISTART, University of Bologna, Italy

ABSTRACT: The paper presents the results of the numerical analyses carried out with the well-known FE code PLAXIS to simulate the response of a 1g small-scale model wall reinforced with polypropylene geogrids, under loads applied on top of the sand bed behind the wall. The capability and reliability of the numerical code to describe the measured behaviour is discussed, particularly with reference to the most suitable material model and parameters. A good general agreement between experimental data and numerical results is shown, especially when considering the complexity of the physical system, characterized by an initially low stress level combined with a highly confined soil-geogrids-wall interaction.

1 INTRODUCTION

The ever increasing use of commercial numerical codes in geotechnical engineering practice urgently demands for new and accurate experimental work, in order to evaluate the applicability and reliability of these codes to describe the behaviour of structures interacting with the soil such as, for instance, shallow and deep foundations, embankments, tunnels or various types of walls.

A special case of wall is represented by the geosyntetic-reinforced walls, whose use is rapidly increasing due to its construction simplicity and flexibility coupled with the low cost of the reinforcement technique. In fact, several types of geotextiles and geogrids, made up of various polymers, are today produced and used as reinforcements.

Small-scale 1g physical models represent a useful tool to reproduce the behaviour of such reinforced structures and already provided a rational basis for most calculation methods (e.g. Juran & Christopher, 1989; Palmeira & Lanz, 1994; Helwany & Wu, 1995; Karpurapu & Bathurst, 1995), but their direct application to design purposes is still rather limited by the fact that some important similarity requirements are not satisfied.

However, the results of 1g models can be of great benefit for the calibration of the relevant analytical and numerical models (Simonini, 1996), due to their controlled and repeatable test conditions. A rather new experimental research was recently carried out at the University of Padova (Italy), concerning the behaviour of walls reinforced with polypropylene geogrids; some experimental results – especially focused on time and temperature effects - were already published and discussed elsewhere (Gottardi & Simonini, 1997, 2000; Simonini et al. 2000).

In this research - besides a brief presentation of the physical model wall - the results of the experimental study were used to check the capability and the effectiveness of the well-known numerical code PLAXIS (1998) to describe the response of such a rather complex system.

2 THE PHYSICAL MODEL

The physical model wall (1200 mm long, 400 mm wide and 600 mm high) intends to reproduce a plain strain state within the reinforced soil mass. Figure 1 shows a general view of the small-scale model, where the main components - lateral walls, facing elements, reinforced soil and loading plate - can be observed.

The retaining wall is made up of a set of rigid metallic strips, hinged each other and kept vertically only by the interposition of the geogrid layers. The geogrid (1200 mm long and 400 mm wide) are locked into the facing strips and spaced 70 mm. The wall is constructed from bottom to top by anchoring the metallic strips to a provisional vertical track, which is removed after the wall construction is completed. The sand layers are prepared by raining technique. All mechanisms for sand deposition are fully automatic and allow for the achievement of homogeneous and highly reproducible layers, the standard deviation of relative density (85%) being less than 1%.

The reinforced retaining wall is loaded, through a rigid steel plate (200 mm x 400 mm) resting on top of the sand surface, by an electrical stepper motor.

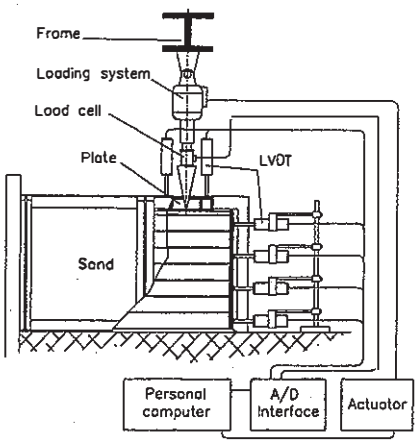

Figure 1. Model wall lay-out.

The load or displacement path generation and the data acquisition from all measurement devices are fully automatic via a personal computer and an A/D interface. The selected position of the displacement transducers allows for the continuous monitoring of the horizontal movements of the wall and the vertical displacement and rotation of the plate.

3 SAND AND GEOGRID PROPERTIES

The soil used for layers preparation is a medium-fine quartz river sand with mean particle size $D_{50} = 0.42$ mm; non-uniformity coefficient $C_u = 2.0$; specific gravity $G_s = 2.71$, minimum and maximum dry unit weight 13.6 e 16.5 kN/m^3.

In order to evaluate the stress-strain behaviour of the sand, isotropically consolidated and drained (CID) triaxial compression tests were carried out on large diameter samples reconstructed by raining technique at the same relative density of 85%.

The deviatoric stress (σ_a - σ_r) vs. axial strain ε_a and the volumetric strain ε_v vs. ε_a curves are plotted in Figure 2. As expected, the dense sand showed a strongly dilatant response under shear. Due to the presence of dilation, the peak-strength envelope is slightly curved and characterized by friction angles decreasing from 42.6° to 41.2° in the range of the investigated stresses. The critical shear strength angle of the sand, estimated from CIU triaxial compression tests, is 33°.

As reinforcing material, a suitably scaled polypropylene geogrid was used (grid size: 12 mm x 14 mm; mass per unit area: 63 g/m^2; tensile strength: 4.5 kN/m). Results of elongation tests, carried out with different strain rates, are reported in Figure 3.

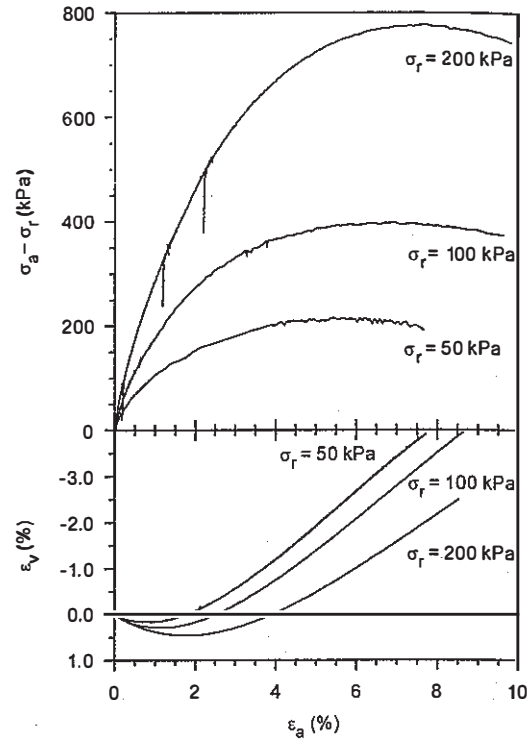

Figure 2. Triaxial tests on large diameter sand samples.

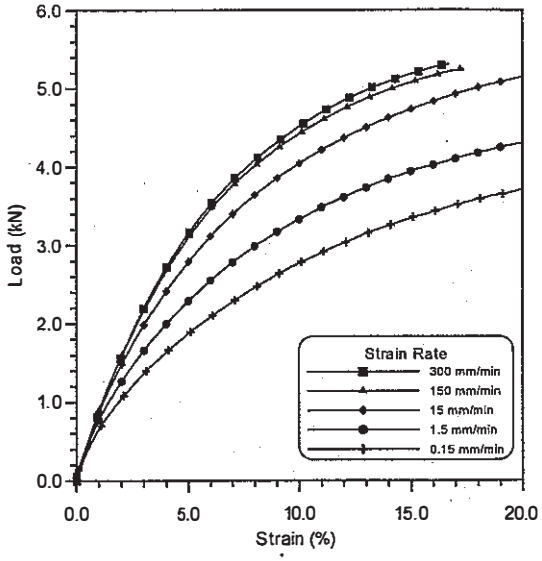

Figure 3. Results of elongation tests on the geogrids.

4 EXPERIMENTAL RESULTS

In the test used to calibrate the numerical analyses the load was applied on top of the sand bed behind the wall, with a constant loading rate of $5 \cdot 10^{-2}$ kN/s, up to failure. Unloading-reloading cycles with an

amplitude of 5 kN were interposed at increasing load levels. Failure was characterised by the collapse of the reinforced wall due to the progressive breakage of the polymeric grids.

Figure 4 provides the results of the relationship between the applied load Q and the vertical displacement of the plate w.

A similar kind of information, related to the wall movements, is provided in Figure 5, where the measurements from all the horizontal transducers are plotted together, in order to provide the deformed configuration at various load levels. Dashed lines represent the position of the reinforcements.

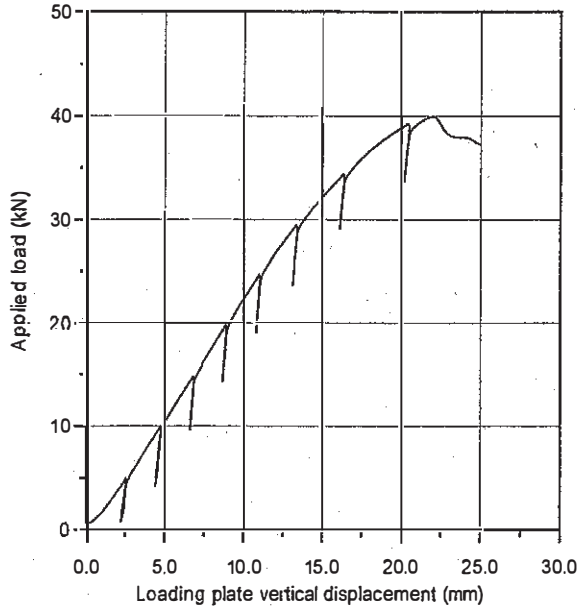

Figure 4. Load-displacement curve of the loading plate.

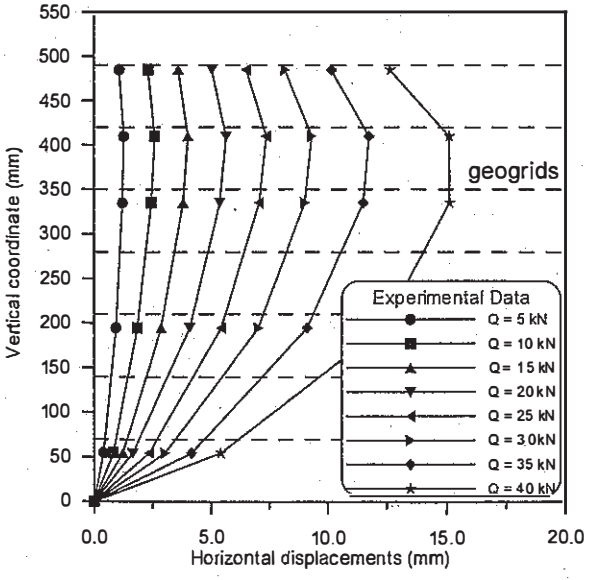

Figure 5. Measured wall deformation at different load levels.

5 PLAXIS ANALYSES

The reinforced wall was schematised with the 2D mesh of Figure 6, with six-node triangular elements for the soil, geogrid elements and hinged beams as wall facing on the right-hand side. No interface was inserted at the beam-soil contact, since it turned out to be not particularly important in this case. The geogrid elements were fixed to the relevant beam hinge, in order to simulate the effect of an anchor to the facing elements. The loading plate was composed of rigid beam elements with a fully rough interface. Horizontal and vertical displacements were restrained at the base of the wall, whereas vertical displacements were free at the left boundary of the mesh. A K_0 initial stress state due to a self-weight γ = 16.0 kN/m^3 was assumed in all the simulations.

The most suitable selection of the material model and related parameters for the various elements forming the reinforced wall was first analysed.

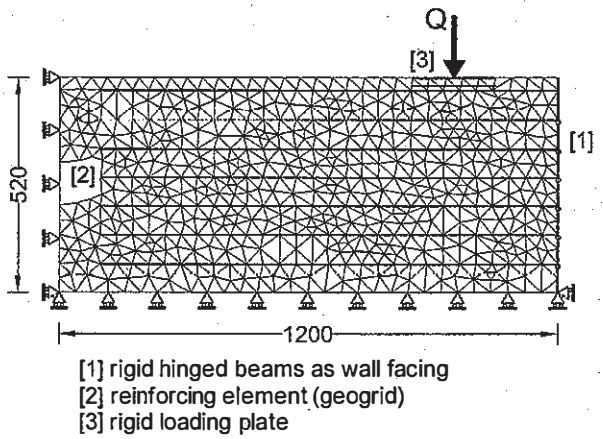

Figure 6. FEM mesh used in the numerical analyses.

5.1 *Material models*

The behaviour of the dense sand was modelled by using both available elasto-plastic constitutive laws implemented in the code, namely the bilinear elastic-perfectly plastic model and an advanced constitutive law, referred as *hardening-soil* model. At failure, both material models are based on the classic Mohr-Coulomb strength criterion, with the possibility of having a non-associated flow, with dilatancy ψ different from the shear strength angle ϕ.

The response of geogrids is linearly elastic: the PLAXIS geosynthetic elements in the basic formulation do not allow to take into account any tensile strength limit.

In order to estimate the strength parameters of the sand, the results of triaxial compression tests shown in Figure 2 were used, whereas the geogrid properties were determined from the elongation tests reported in Figure 3.

Table 1. Material parameters.

SAND STRENGTH			
ϕ' (°) 42	c' (kPa) 2.0	ψ (°) 9	
GEOGRID STIFFNESS			
EA (kN/m)		55	
WALL FACING STIFFNESS			
E (GPa) 2.06		ν 0.30	

A summary of the adopted material parameters is reported in Table 1. A small cohesion was introduced in order to avoid possible numerical instabilities and excessive computational times. The sand constant stiffness modulus required by the elastic-perfectly plastic material model was obtained via back-analyses of the experimental data. The numerical output of the overall response of the wall proved, as expected, to be very sensitive to such parameter, assumed equal for all the FE elements. An elastic modulus of 6.5 MPa was found to provide a good agreement in terms of applied load-vertical displacement curve (see Figure 8).

The basic feature of the advanced *hardening-soil* model, based on the hyperbolic approximation of the soil response under shear, is the stress-dependency of the soil stiffness. Therefore, no back-analysis was required in this case and the relevant stiffness parameters could be independently determined on the basis of the results of the triaxial compression tests already described in Section 3. In addition, plastic strains due to both the deviatoric and the hydrostatic stress increments can be taken into account. The complete description of the *hardening-soil* model can be found in the PLAXIS user manual.

Table 2 summarizes the stiffness parameters used with the two material models (p'_{ref}=100 kPa).

Table 2. Stiffness parameters of the soil material models.

ELASTIC-PERFECTLY PLASTIC MODEL			
E (MPa)	6.50	ν	0.20
HARDENING-SOIL MODEL			
E_{50}^{ref} (MPa)	16.35	E_{ur}^{ref} (MPa)	65.40
E_{oed}^{ref} (MPa)	20.67	ν_{ur}	0.20
m	0.62	R_f	0.9

5.2 *Validation of the hardening-soil model*

A preliminary check of the effectiveness of the *hardening-soil* model to reproduce the behaviour of the dense sand was first carried out, simulating with PLAXIS the CID triaxial compression tests.

Figure 7 compares the experimental and the simulated (dashed lines) response in both (σ_a - σ_r) vs. ε_a and ε_v vs. ε_a planes. Note the good agreement between experimental curves and numerical simulations, especially in the deviatoric stress – axial strain plane. Assuming a dilatancy angle of only 9° (and $\phi_{cr} \simeq 33°$), the volumetric strains turn out to be underestimated.

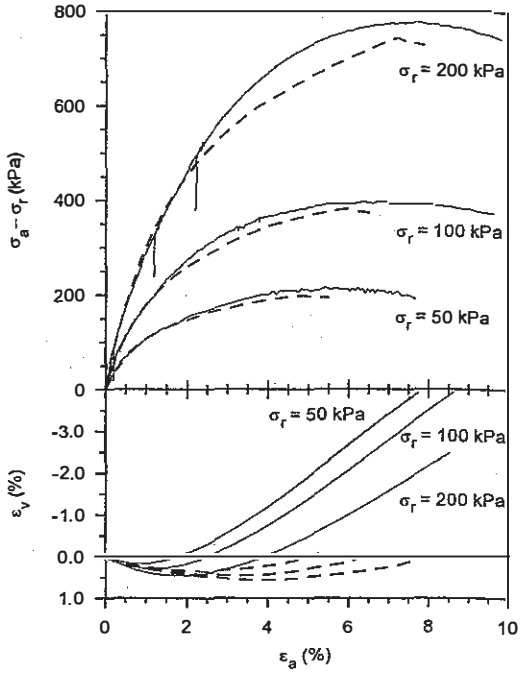

Figure 7. Triaxial tests on sand: comparison between experimental data and numerical simulations.

5.3 *Model wall simulation*

In order to reproduce the wall response, vertical displacements were applied at the nodes of the top plate. The final displacement of 20 mm (equivalent to the physical model failure) was given in 416 increments, with a relative error tolerance in each computational step of 0.003. The main outcome of the analyses, to be compared with the measured curve of the top plate applied load-vertical displacement, is plotted in Figure 8.

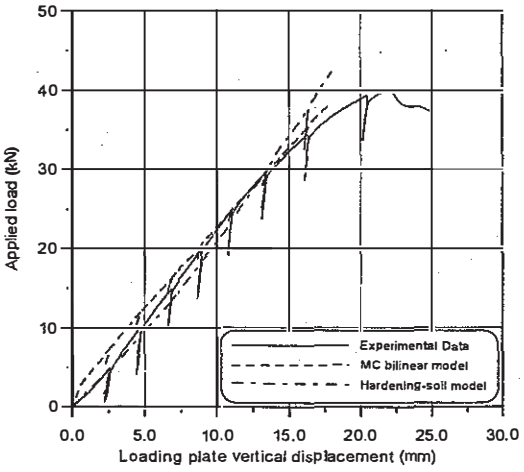

Figure 8. Load vs. vertical displacement of the top plate: comparison between experimental data and numerical simulations.

Apart from the final, fragile failure of the physical system, shown by the peak load in the experimental curve and by the formation of a clear mechanism inside the reinforced soil, which cannot be reproduced in such numerical analyses, there is a substantial good agreement between the experimental data and both numerical models used, especially when considering the hardening-soil model, which seems to be able to reproduce the softer wall behaviour at lower load levels.

It is interesting to observe that, whereas the results of the MC bilinear model are essentially a good fit of the experimental data, the prediction with the hardening-soil model was obtained using the material parameters independently determined with actual element tests (i.e. triaxial tests for sand and elongation tests for geogrids).

Such results comparison is well summarised in Figure 9, which shows the wall deformation at the maximum load level and at half-way to it. The numerical model is not able to reproduce the top reinforcement layer slippage, which is in fact a clear feature of the physical model. However, the hardening-soil model seems to better capture the larger horizontal displacements at higher stress levels.

Displacement vectors, computed at 20 mm of vertical displacement of the top plate, are plotted in Figures 10a and 10b. Note the general trend inside the reinforced soil mass and behind the wall, that confirms the trend of the horizontal wall displacements of Figure 9. No strain localisation along a well defined sliding surface, as clearly noticed in the physical model, is possible in these numerical analyses.

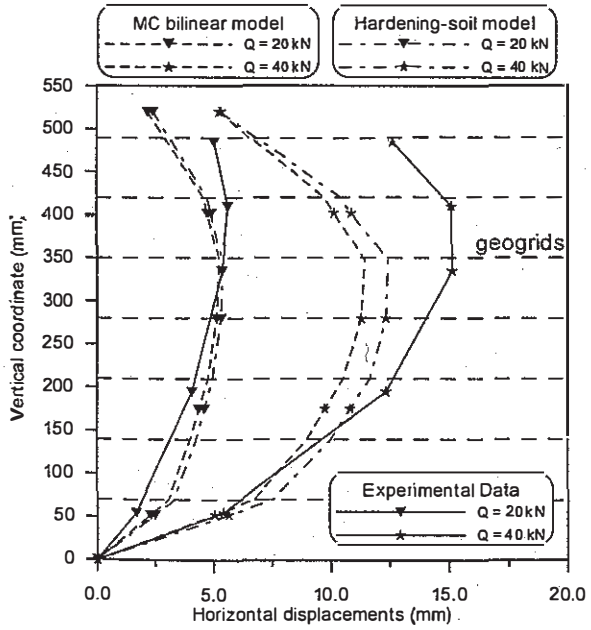

Figure 9. Wall displacements: comparison between experimental data and numerical simulations.

Figures 11a and 11b show the distribution of the tensile forces along the geosynthetics at the same final situation. The greatest values are observed in the third and fourth layer (from top), in correspondence of the maximum lateral wall movements, the maximum tensile force being equal to 2.30 kN/m. The general pattern corresponds to what observed in the physical model, except for the already noticed slippage of the shallowest reinforcement layer.

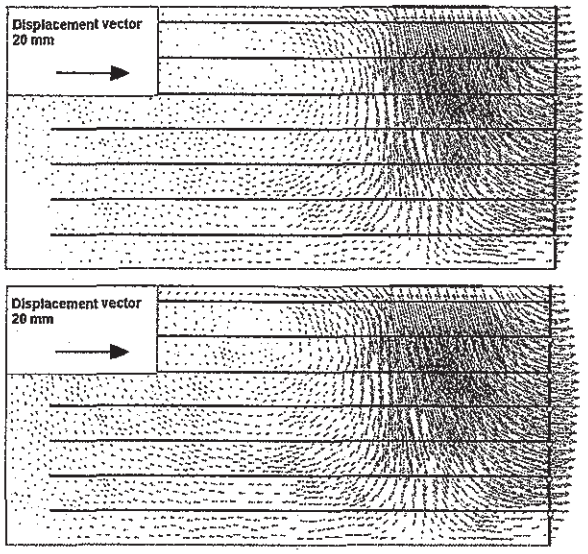

Figure 10. Displacement vectors: a) MC bilinear model; b) Hardening-soil model.

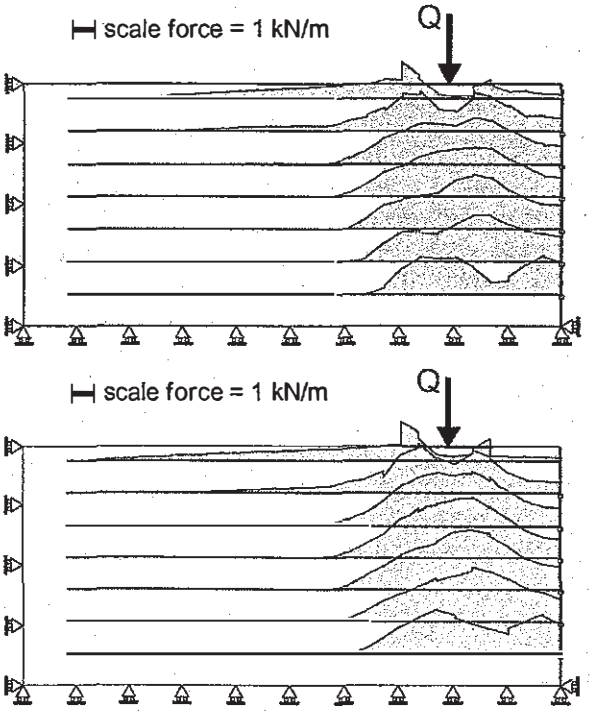

Figure 11. Tensile forces in the reinforcements: a) MC bilinear model; b) Hardening-soil model.

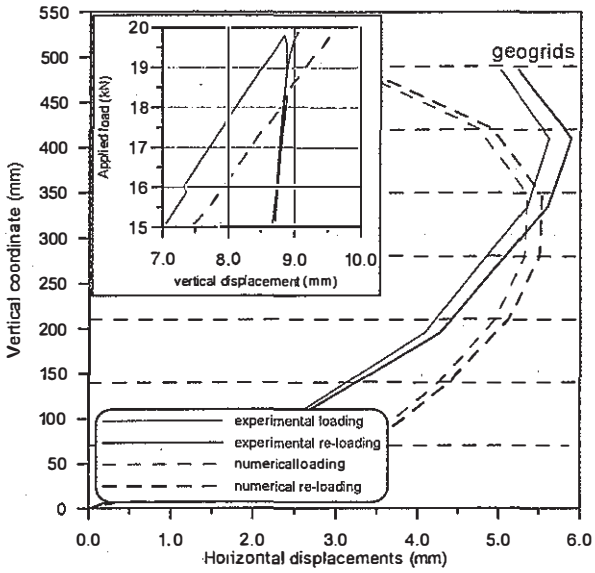

Figure 12. Loading-unloading-reloading cycle at Q = 20 kN.

Finally, with respect to the classic MC bilinear model, the hardening-soil model seems to be more able to reproduce the actual unloading-reloading response. The typical behaviour is presented with reference to the unloading-reloading cycle displayed in the upper-left part of Figure 12 (between 15 and 20 kN). Note the very good agreement of the numerical results. The deformed shape of the wall is also reported at the end of each loading cycle.

6 CONCLUSIONS

The present research was aimed at testing the effectiveness of the well-known FE code PLAXIS when reproducing the behaviour of a small-scale reinforced wall, loaded up to a stress level corresponding to the failure onset in the physical model. The reinforced system is made up of a very dense dilating sand, initially at a very low stress level, and heavily confined geogrids connected to stiff facing elements.

Two suitable constitutive models implemented in the code were used to describe the soil behaviour, namely the classic Mohr-Coulomb, bilinear model and an advanced hardening-soil model. With the latter it was possible to introduce the stress-dependency of soil stiffness and the actual unloading-reloading sand response. Most important, only with the hardening model it was possible to introduce the soil parameters as deduced from specifically performed standard compression triaxial tests.

Both numerical simulations showed a remarkable good agreement with the experimental trend of the vertically loaded top plate. As regards the wall deformation, neither type of analysis can reproduce the slippage of the top reinforcement layer, which is in fact a constant feature of the physical model.

Furthermore, in both cases it was observed that the tensile forces in the geogrids at the maximum applied load remained relatively distant from the ultimate strength and thus cannot explain the actual occurrence of the sudden and catastrophic collapse of the model wall, caused by the progressive breakage of the reinforcements. This difference could be partially explained when we consider that the FE code and the constitutive models used do not take into account the material softening and the strain localisation - and the consequent stress concentration - along a well defined sliding surface.

REFERENCES

Gottardi, G., Simonini, P. 1997. Long term behaviour of reinforced walls: model results. *Proc. Int. Conf. Geosynthetics Asia '97*, Vol. 2: 43-50. Bangalore, India, November 1997.

Gottardi, G., Simonini, P. 2000. Time and temperature effects on the behavior of geogrid reinforced walls. *Proc. 2th Eur. Geosynthetics Conference*, EUROGEO 2000, Bologna, Vol. 1: 175-180. Patron Editore, Bologna.

Helwany, M.B., Wu, J.T.H. 1995. A numerical model for analyzing long-term performance of geosynthetic-reinforced soil structures. *Geosynthetics International*, Vol. 2, N. 2: 429-453.

Juran, I., Christopher, B. 1989. Laboratory model study on geosynthetic reinforced soil retaining walls. *Journal of Geot. Eng., ASCE*, 115, N. 7: 905-926.

Karpurapu, R., Bathurst, R.J. 1995. Behaviour of geosynthetic reinforced soil retaining walls using the finite element method. *Computer and Geotechnics*, 17: 279-299.

Palmeira, E.M., Lanz, D. 1994. Stresses and deformations in geotextile reinforced model walls. *Geotextiles and Geomembranes*, 13: 331-348.

PLAXIS - Finite Element Code for Soil and Rock Analyses. 1998. Version 7. Netherlands: PLAXIS B.V.

Simonini, P. 1996. A finite element approach to the strength of granular soils reinforced with geosynthetics. *Proc. of the International Symposium on Earth Reinforcement*: 675-680. Fukuoka, Kiushu, Japan, 12-14 November 1996.

Simonini, P., Schiavo, M., Gottardi, G. & Tonni, L. (2000). Numerical analysis of a model wall reinforced with polypropylene geogids. *Proc. 2th Eur. Geosynthetics Conference*, EUROGEO 2000, Bologna, Vol. 1: 231-236. Patron Editore, Bologna.